Circular-Pad via Model Based on Cavity Field Analysis

G. A. Kouzaev, N. K. Nikolova, *Member, IEEE*, and M. J. Deen, *Fellow, IEEE*

***Abstract*—An equivalent circuit model of a circular-pad grounding via is proposed based on cavity modal analysis. The modes of the via are derived analytically. Each mode is represented by an equivalent circuit taking into account ohmic losses, as well as losses due to spatial and surface wave radiation. It is shown that the degradation of grounding via characteristics at high frequencies is caused by the multimode effects and radiation. The accuracy of the proposed semi-analytical via model is comparable with that of full-wave analysis up to 75 GHz. It is fast and is easily incorporated in high-frequency circuit simulators.**

***Index Terms*—Equivalent circuits, physics based models, vias.**

I. INTRODUCTION

VIAS connecting two or more metal layers are important components in the contemporary high-density integrated circuits [1][2]. At high frequencies, diffraction, resonances, and losses substantially distort their characteristics and limit the rate of high-speed signals [1]–[4]. The complex electromagnetic (EM) nature of the effects is not properly represented in any of the currently available equivalent circuits (ECs) of vias. The general purpose 3-D EM solvers can offer adequate modeling. However, they require long computation times and the results are valid only for the specific substrate and dimensions.

This letter describes an EC model for circular-pad grounding vias (see Fig. 1) based on the analytical equivalent-cavity approach. Our model takes into account ohmic and radiation losses. The model is verified with results obtained for large concentrically-shorted circular-patch microstrip antennas, which have the same geometry and the same significant EM effects [5], [6]. Our analytical model is also in good agreement with Agilent Momentum [7] simulations.

II. THEORY

A. Cavity Model of a Circular-Pad Via

The circular pad via is modeled with an equivalent cavity formed by a cylindrical magnetic wall. The wall has an effective radius R_e, greater than the via-pad radius R_b due to the fringing effect [see Fig. 1(a)]. The top wall of the cavity is a perfect conductor representing the extended circular via-pad. The field vectors $\mathbf{E}$ and $\mathbf{H}$ are expanded in a series of modes ; e.g., $\mathbf{E} = \sum_{n,m,k}^{\infty} a_{nmk}\mathbf{E}_{nmk}$, where a_{nmk} are the amplitudes of the modes. The subscripts m, n and k correspond to the respective eigenvalues in the solution of the Helmholtz equation.

Manuscript received January 2, 2003; revised June 30, 2003. The review of this letter was arranged by Associate Editor Dr. Arvind Sharma.

The authors are with the Department of Electrical and Computer Engineering, McMaster University, Hamilton, ON L8S 4K1, Canada (e-mail: talia@mcmaster.ca).

Digital Object Identifier 10.1109/LMWC.2003.818519

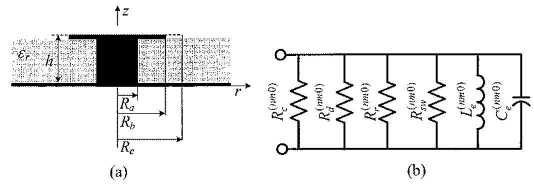

Fig. 1. Grounding via (a) and a resonant modal equivalent circuit (b).

Consider only the TM_z. The normal-to-the-substrate magnetic field H_z is zero, and E_z does not vary with z (i.e., $k = 0$):

$$E_z = \sum_{n,m}^{\infty} E_{z_{nm0}},$$
$$E_{z_{nm0}} = [A_{nm0}J_n(k_c r) + B_{nm0}Y_n(k_c r)]\cos n\varphi \quad (1)$$

where A_{nm0} and B_{nm0} are the unknown modal amplitudes; J_n and Y_n are Bessel and Neumann functions of order n ($n = 0, 1, \ldots$), n being the number of field variations in the φ-direction; $k_c = (\omega/c)\sqrt{\varepsilon_r}$, ω being the angular frequency, c is the velocity of light, and ε_r is the substrate relative permittivity. The angular component $H_{\varphi nm0}$ is derived from $E_{z_{nm0}}$. The boundary conditions

$$E_{z_{nm0}}(r = R_a) = 0 \quad \text{and} \quad H_{\varphi_{nm0}}(r = R_e) = 0 \quad (2)$$

hold at the surface of the perfectly conducting via rod $(r = R_a)$ and at the magnetic wall $(r = R_e)$. They are used to obtain the eigenvalue equation

$$J_n(k_c R_a)Y_n'(k_c R_e) – J_n'(k_c R_e)Y_n(k_c R_a) = 0, \quad n = 0, 1, 2, \ldots \quad (3)$$

from which the resonant frequencies are computed. Here, J_n' and Y_n' are the derivatives of the Bessel and Neumann functions, respectively. Equation (2) also allows for the derivation of the unknown coefficients A_{nm0} and B_{nm0}. The TM_{nm0} mode corresponds to the m-th root ω_{nm0} of the n-th equation in (3). Here, $m(m = 1, 2, \ldots)$ corresponds to the number of field variations along r.

We describe each mode of the via by an EC composed of a capacitor, an inductor, and resistors representing the via loss [Fig. 1(b)]. The modal capacitance $C_e^{(nm0)}$ and inductance $L_e^{(nm0)}$ are derived using the stored energy of the electrical field $W_e^{(nm0)}$ and the modal voltage V_{edge} between the pad edge and the ground plane at the resonant frequency ω_{nm0} [8]

$$C_e^{(nm0)} = \frac{2W_e^{(nm0)}}{V_{edge}^2}; \quad L_e^{(nm0)} = \frac{1}{C_e^{(nm0)}\omega_{nm0}^2}. \quad (4)$$

The zero-frequency mode of the via cavity is added to the expansion (1) for completeness. In the EC, this mode is represented by an equivalent inductor $L^{(0)}$, which must be connected in series with the modal EC in Fig. 1(b). An approximate expression for $L^{(0)}$ is provided in [4]:

$$L^{(0)} = \frac{\mu_0}{2\pi}\left[h \ln\left(\frac{h+\sqrt{R_a^2+h^2}}{R_a}\right) + \frac{3}{2}\left(R_a - \sqrt{R_a^2+h^2}\right)\right]. \quad (5)$$

B. Via Loss Calculation

The conductor equivalent resistance R_c is calculated by the substitution of the loss-free via cavity results into the perturbation formula [6]

$$R_c^{(nm0)} = \frac{0.25 h V_{edge}^2}{\omega_{nm0} W_m^{(nm0)} \sqrt{0.5\mu_0 \omega_{nm0}\sigma}} \quad (6)$$

where $W_m^{(nm0)}$ is the magnetic field energy and σ is the specific conductivity of the via conductor. The equivalent resistor is connected in parallel with the modal equivalent tank as shown in Fig. 1(b). The conduction loss resistance for the static magnetic mode is negligible and it is not taken into account.

The dielectric loss is represented by an equivalent resistor in parallel (see Fig. 1(b)), calculated by a perturbation formula [8]

$$R_d^{(nm0)} = \frac{0.25 V_{edge}^2}{\omega_{nm0} W_e^{(nm0)} \tan\delta}. \quad (7)$$

In (7), $\tan\delta$ is the dielectric loss tangent.

The via cavity edge voltage V_{edge} and the modal resonant frequency ω_{nm0} are used to derive the radiated fields, from which the equivalent radiation resistance $R_r^{(nm0)}$ is calculated [9]:

$$R_r^{(nm0)} = \frac{1}{G_r^{(nm0)}},$$
$$G_r^{(nm0)} = \delta_{n0}\frac{(k_{mn0}R_e)^2}{480} \times \int_0^{\frac{\pi}{2}} \left[B_M^2(X) + B_P^2(X)\cos^2\theta\right]\sin\theta d\theta \quad (8)$$

where

$$B_P(X) = J_{n-1}(X) + J_{n+1}(X),$$
$$B_M(X) = J_{n-1}(X) - J_{n+1}(X),$$
$$X = k_{nm0} R_e \sin\theta,$$
$$\delta_{n0} = \begin{cases} 2, & n = 0 \\ 1, & n \neq 1 \end{cases}.$$

In (8), θ denotes the elevation angle in the spherical coordinate system, and $k_{nm0} = \omega_{nm0}/c$. The formula above is valid for electrically thin substrates and TM modes.

Another effect relates to surface wave radiation. The equivalent resistance $R_{sw}^{(nm0)}$ is computed as [10]

$$R_{sw}^{(nm0)} = \frac{1}{2}\frac{V_{edge}^2}{P_{sw}} \quad (9)$$

TABLE I
COMPARISON OF THE MEASURED [14] AND CALCULATED RESONANT FREQUENCY OF THE TM_{110} MODE OF A MICROSTRIP CIRCULAR PATCH

Sample number	R_b (mm)	h (mm)	ε_r	f_{110} (GHz) measured	f_{110} (GHz) our result	Error (%)	f_{110} (GHz) Chew's formula [12]	Error (%)
1	1.9698	0.4900	2.43	25.600	25.7447	0.56	24.0107	6.41
2	3.9592	0.4900	2.43	13.100	13.4911	2.94	12.8787	1.70
3	5.8898	0.4900	2.43	8.960	9.2285	2.95	8.9027	0.64
4	8.0017	0.4900	2.43	6.810	6.8581	0.70	6.6609	2.21
5	9.9617	0.4900	2.43	5.470	5.5380	1.24	5.4013	1.26
6	4.7752	1.1938	10.00	5.455	5.2326	4.16	5.1430	5.89
7	7.1628	1.1938	10.00	3.650	3.6010	1.10	3.5609	2.47

where

$$P_{sw} = \delta_{n0}\frac{V_{edge}^2}{240}\pi R_e^2 k_{nm0}^2 \left[J_n'(\chi R_e)\right]^2 \times \mathrm{tnc}^2(k_{z1}h)F(h) \quad (10)$$

$$F(h) = \left[\frac{1}{|k_{z0}h|} + \frac{1+\mathrm{snc}(2k_{z1}h)}{\varepsilon_r \cos^2(k_{z1}h)}\right]^{-1} \quad (11)$$

$$\mathrm{snc}(x) = \frac{\sin(x)}{x}, \quad \mathrm{tnc}(x) = \frac{\tan(x)}{x}. \quad (12)$$

The unknown radial propagation constant χ of the dominant surface mode is obtained from the eigenvalue equation [11]

$$\frac{1}{k_{z0}} = \frac{\varepsilon_r \tan(k_{z1}h)}{k_{z1}};$$
$$k_{z0} = \sqrt{k_{nm0}^2 - \chi^2},$$
$$k_{z1} = \sqrt{k_{nm0}^2\varepsilon_r - \chi^2}. \quad (13)$$

III. NUMERICAL RESULTS

A. Modal Resonant Frequencies

The modal resonant frequencies of the via are calculated using (3) where we need the value of the effective radius of the mode. The edge capacitance of a via is similar to that of a circular microstrip patch. There are few semi-empirical or approximate formulas in the literature for the calculation of the effective radius or capacitance of circular patches printed on grounded dielectric substrates [12]. We have modified a formula for the effective extension of the edge of a triplate waveguide [13] by curve-fitting technique according to experimental data for circular microstrip patches [14]–[16]. We obtain first-order approximate formulas for the effective modal radii:

$$R_e^{(nm0)} = R_b + 0.553h, \quad n = 0 \quad (14)$$
$$R_e^{(nmo)} = R_b + 0.45h, \quad n \geq 1. \quad (15)$$

To verify (14) and (15), we have calculated the resonant frequencies of microstrip circular patch resonators for different substrates and for frequencies up to 26 GHz according to

$$\omega_{nm0} = \frac{k_{nm0}c}{\left(R_e^{(nm0)}\sqrt{\varepsilon_r}\right)}. \quad (16).$$

The results agree well with experimental data provided in [14]–[16] for a number of substrates and modes. In Table I, we summarize the comparison with the data of Losada *et al.* [14] for the resonant frequencies of the TM_{110} mode. In summary, it has been found that (14)–(16) provides several percent error

TABLE II
COMPARISON OF THE MEASURED [5] AND CALCULATED MODAL RESONANT FREQUENCIES OF A CONCENTRICALLY SHORTED (VIA-LIKE) RESONATOR

Mode	f_{nm0} (GHz) measured	f_{nm0} (GHz) our result	Error (%)	f_{nm0} (GHz) Chew's formula [12]	Error (%)
TM_{010}	0.165	0.1598	3.20	0.1566	5.22
TM_{110}	0.385	0.3834	0.42	0.3749	2.66
TM_{210}	0.646	0.6352	1.69	0.6216	3.85
TM_{310}	0.899	0.8737	2.85	0.8550	5.01
TM_{410}	1.101	1.1059	0.44	1.0821	1.73

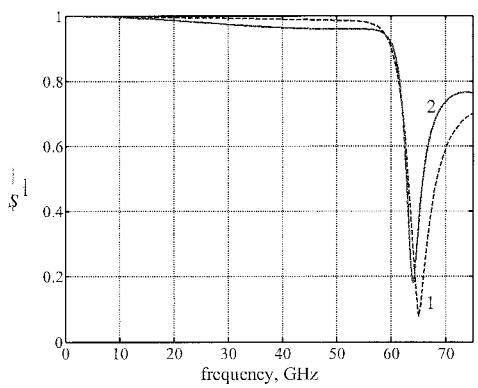

Fig. 2. Reflection coefficient of a grounding via: 1—Momentum results, 2—proposed model. Via parameters: $R_a = 0.152$ mm, $R_b = 0.3302$ mm, $h = 0.254$ mm, $\varepsilon_r = 9.9$.

in the calculation of the resonant frequencies if the substrate dielectric permittivity is in the range of $2.32 \leq \varepsilon_r \leq 10$. The substrate height should be comparable or smaller than the patch radius, $R_b/h \geq 1$; and it must be electrically small, $k_{nm0}h < 1$. In this range, similar accuracy is achieved with Agilent's Momentum [7].

Utilizing our effective radius formulas, we now compute the resonant frequencies of a via cavity using a Matlab search algorithm applied. These results are verified by measurement data for concentrically-shorted circular-patch antennas, which have the same geometry as the via. A comparison with the results provided in [5] is summarized in Table II ($R_a = 2.5$ mm, $R_b = 142.5$ mm, $h = 6$ mm, $\varepsilon_r = 2.5$). The error does not exceed 3.2% and is less than the error produced by previously published approximate formulas.

B. Reflection Coefficient Computation for a Grounding Via

The grounding via is excited by a 50-Ω port placed directly at its edge. The field inside the via cavity is composed of multiple modes (1) whose number is limited by achieving a desired convergence. This number increases as the via-pad radius increases. In the case of multiple modes, the via's EC consists of the modal tanks [Fig. 1(b)] and $L^{(0)}$ [see (5)] connected in series.

Here, we use five azimuthal-type modes ($n = 0, \ldots, 4$; $m = 1$) in order to compute the S-parameters of a grounding via. The reflection coefficient is plotted in Fig. 2 together with the results of Momentum. The via is realized on a thin alumina substrate used in high-speed applications because of its good thermal properties. This number of resonant modes provides good convergence of $|S_{11}|$ in a wide frequency range which is limited by the excitation of higher-order modes in the input microstrip line (~78 GHz). The reflection minimum is due mostly to the TM_{010} and TM_{110} modes. The radiation of all modes defines the depth of the minimum and the level of the via performance degradation, which limits the frequency band for high-speed applications.

IV. CONCLUSIONS

A semi-analytical model of a circular-pad grounding via based on the cavity field analysis has been developed. The modal equivalent circuits take into account the conductor and substrate losses, as well as spatial and surface wave radiation. It features high computational efficiency and accuracy in comparison with full-wave EM simulators. The resonant frequencies and the losses of circular-pad vias are also studied. It is found that the performance degradation at high frequencies is due mainly to multimode excitation and radiation losses, which limit the rate of high-speed signals in multilayer circuits to several tens of gigabit per second.

ACKNOWLEDGMENT

The authors thank Dr. A. Rahal for the fruitful discussions of the results.

REFERENCES

[1] Z. Wang, M. J. Deen, and A. Rahal, "Modeling of integrated inductors and resistors for microwave applications," in *Integrated Passive Component Technology*. New York: IEEE Press, 2003, ch. 11.
[2] V. I. Gvozdev, G. A. Kouzaev, E. I. Nefeodov, and V. A. Yashin, "Physical principles of the modeling of three-dimensional microwave and extremely high frequency integrated circuits," *Soviet Phys.—Uspekhi*, vol. 35, pp. 212–230, 1992.
[3] S. Maeda, T. Kashiva, and I. Fukai, "Full wave analysis of propagation characteristics of a through hole using the finite-difference time-domain method," *IEEE Trans. Microwave Theory Tech.*, vol. 39, pp. 2154–2159, Dec. 1991.
[4] M. E. Goldfarb and R. A. Pucel, "Modeling via hole grounds in microstrip," *IEEE Microwave Guided Wave Lett.*, vol. 1, pp. 135–137, June 1991.
[5] R. G. Vaughan, "Two-port higher mode circular microstrip antennas," *IEEE Trans. Antennas Propagat.*, vol. 36, pp. 309–321, Mar. 1988.
[6] Y. Lin and L. Shafai, "Characteristics of concentrically shorted circular patches," *Proc. Inst. Elect. Eng.*, vol. 137, pp. 18–24, Feb. 1990.
[7] *Advanced Design System 2002, Momentum*. Palo Alto, CA: Agilent Technologies, 2002.
[8] T. Okoshi, *Planar Circuits for Microwaves and Light Waves*. Berlin, Germany: Springer Verlag, 1985.
[9] A. G. Derneryd, "Analysis of the microstrip disk antenna element," *IEEE Trans. Antennas Propagat.*, vol. 27, pp. 660–664, Feb. 1979.
[10] D. R. Jackson, J. T. Williams, A. K. Bhattacharyya, R. L. Smith, S. J. Buchheit, and S. A. Long, "Microstrip patch designs that do not excite surface waves," *IEEE Trans. Antennas Propagat.*, vol. 41, pp. 1026–1037, Aug. 1993.
[11] T. Itoh, Ed., *Numerical Techniques for Microwave and Millimeter Wave Passive Structures*. New York: Wiley, 1989.
[12] W. C. Chew and J. A. Kong, "Effects of fringing fields on the capacitance of circular microstrip disk," *IEEE Trans. Microwave Theory Tech.*, vol. 28, pp. 98–104, Feb. 1980.
[13] N. Marcuvitz, *Waveguide Handbook*. London, U.K.: Peter Peregrinus, 1993.
[14] V. Losada, R. R. Boix, and M. Horno, "Resonant modes of circular microstrip patches in multilayered substrates," *IEEE Trans. Microwave Theory Tech.*, vol. 47, pp. 488–497, Apr. 1999.
[15] J. S. Dahele and K. F. Lee, "Theory and experiment on microstrip antennas with airgaps," *Proc. Inst. Elect. Eng.*, vol. 132, pp. 455–460, Dec. 1985.
[16] Y. T. Lo, D. Solomon, and W. Richards, "Theory and experiment on microstrip antennas," *IEEE Trans. Antennas Propagat.*, vol. 27, pp. 137–145, Feb. 1979.